

Insight into bubble nucleation at high-pressure drop rate

Daniele Tammaro¹, Salvatore Iannace² and Ernesto Di Maio¹

Journal of Cellular Plastics

0(0) 1–10

© The Author(s) 2017

Reprints and permissions:

sagepub.co.uk/journalsPermissions.nav

DOI: 10.1177/0021955X17695094

journals.sagepub.com/home/cel



Abstract

This paper presents insight in bubble nucleation in polymer foaming with physical blowing agent using a batch foaming technique. In our experiments the bubble nucleation is triggered by a sudden pressure drop that causes the supersaturation in the polymer gas solution. In fact, the pressure drop rate is an important process variable since it plays a role in both bubble nucleation and growth. Herein, we investigated very high pressure drop rates, and confirmed the great importance of the pressure drop rate as foaming process variable. The results show that the number of nucleated bubbles increases of one order of magnitude and the foam density is reduced if the pressure drop rate is increased from 50 to 500 MPa/s. Interestingly, the number of nucleated bubble increases linearly in a bi-logarithmic scale as function of pressure drop rate at all the investigated temperatures. Moreover, in the current paper, it is discussed how talc used as nucleating agent plays a role in cooperation with pressure drop rate on bubble nucleation at different foaming temperatures.

Keywords

Nucleation, pressure drop rate, polystyrene, CO₂, foam density

Introduction

Polymeric foams are ubiquitous in our life and in any industrial field, for their excellent acoustic and thermal insulating properties and for specific mechanical

¹Dipartimento di Ingegneria Chimica, dei Materiali e della Produzione Industriale, University of Napoli Federico II, Napoli, Italy

²Istituto per lo Studio delle Macromolecole, Consiglio Nazionale delle Ricerche, Milano, Italy

Corresponding author:

Daniele Tammaro, Dipartimento di Ingegneria Chimica, dei Materiali e della Produzione Industriale, University of Napoli Federico II, Ple Tecchio 80, I-80125 Napoli, Italy.

Email: daniele.tammaro@unina.it

properties.¹ The pressure drop rate, PDR, defined as the rate at which the blowing agent pressure is released from the saturation pressure to ambient pressure after the solubility has been reached, is an important processing variable¹ in thermoplastic gas foaming, being involved in the competition between the bubble nucleation and growth.^{2,3} Different final foam morphologies with different properties can be obtained by properly tuning the PDR. In particular, fine-celled foams can be produced. They exhibit higher mechanical properties and better thermal insulation properties with respect to coarse-celled foams, and are used in a multitude of different applications, including transportation, construction, packaging, food, extraction, and separation.³ Guo et al.⁴ investigated the effect of PDR on the bubble nucleation in a pressure-induced foaming process and designed a batch foaming system to “online” visualize the bubble nucleation phenomenon according in a transparent polymer disc. The results show, on the polystyrene (PS)/carbon dioxide (CO₂) system, that higher density of nucleated bubbles (N), higher nucleation rate and smaller induction time are observed when the PDR increases. Park et al.⁵ studied the effect of PDR on continuous foaming processes, reporting that the experimental results indicate that both the magnitude and the rate of pressure drop play a strong role in the process to induce a microcellular morphology because it affects the thermodynamic instability induced in the polymer/gas solution. Taki⁶ developed a model for the prediction of the bubble nucleation and growth as function of PDR, and validated it with a polypropylene (PP)/CO₂ system. The results of modeling showed an increase of N as function of PDR. In fact, as a general role, the increase of PDR increases the rate of stable nuclei formation, and reduces the chances for the blowing agent to inflate the newly developed bubbles, with a consequent reduction of the mean cell size.^{4,7} The nucleation and growth processes, during the foaming time, compete to consume the excess gas in the system and, if PDR is increased, the nucleation rate is higher and a greater number of cells is formed. In this context, Khan et al.^{8–10} modeled the effect of PDR on bubble nucleation and derived the PDR limit above which N reaches a threshold. In their case, the threshold corresponded to ca. 10 GPa/s, in agreement with the experimental findings in the literature.^{4–6,12} Nevertheless, it is reasonable that the presence of a PDR above which N reaches a threshold depends on the polymer/gas system. The dependence of N at high PDR values and the possible presence of a threshold are both not well understood and are both interesting open problems.

Conventional vessels for polymer batch foaming do not reach very high PDRs. In this context, some of the authors developed a batch foaming equipment, called “minibatch,” to substantially increase PDRs with respect to conventional vessels.¹¹ In the current work, the final foam morphology of PS foams blown with CO₂ on a wide range of PDRs (ranging from 50 to 500 MPa/s) was investigated and the effect of talc as nucleating agent was studied.

Materials and methods

The polymer used is a polystyrene – PS (N2380), supplied by Versalis S.p.A. (Mantova, Italy) having an average molecular weight, density and melt flow index, equal to 300 kDa, 1.05 g/cm³ and 2.0 g/10 min at 200°C and 10 kg, respectively. Talc, supplied by Imerys Talc (Toulouse, France) with mean particle size equal to 1.8 μm was used as nucleating agent at 1% wt with respect to PS content.

PS and talc were dried overnight under vacuum at 90°C, and melt compounded in a co-rotating twin-screw extruder (15 mL Micro Compounder, DSM Xplore, Geleen, The Netherlands). The extrusion process was performed at 210°C and nitrogen as purge gas was used to avoid oxygen and moisture absorption in the hopper. The screw speed was set to 150 rpm, corresponding to an average shear rate of ca. 75 s⁻¹, and the residence time, accurately controlled by means of a backflow channel, was 240 s. The extrudate was granulated for subsequent foaming experiments. After the mixing procedure, the homogeneous dispersion of talc particles in the polymer matrix was confirmed by SEM analysis (data not reported for brevity). CO₂ (99.95% pure) supplied by Sol Group S.p.A. (Monza, Italy) was used as the physical blowing agent.

The foaming apparatus utilized in this study, the minibatch,¹¹ allows to reach PDRs as high as 500 MPa/s from a saturation pressure of 10 MPa, and up to 1800 MPa/s, from a saturation pressure of 30 MPa.

The very high PDR entails some errors in the measurement of pressure. On top of this, for samples having a ratio $\frac{\text{sample surface}}{\text{sample volume}}$ smaller than the samples used in the current work, one expects some delay in the thermal homogenization of the sample. This is more important when using large pressure vessels and large samples, where high PDRs induce large inhomogeneities both in the local PDR experienced by the material and, more importantly, in the resulting temperature gradient in the sample volume. In our case, we have the advantage of the minimization of both the vessel and sample volume and we hypothesize the sample does not experience any thermal and pressure inhomogeneity. In fact, the change of pressure propagates at the speed of sound, which travels in our 1.5-mm thick sample within 10⁻⁵s, while pressure release lasts 10⁻³s. In the case of larger samples (e.g. 10 cm), the two characteristic timeframes could match and PDR effects may possibly reflect in the foaming. Please note that induction time for nucleation is of the order of seconds, in gas foaming of polymers. A possible PDR spatial gradient within the sample may induce a temperature gradient, which, in turn, due to the low thermal conductivity of polymers, will not dissipate during the induction time, with a final spatial inhomogeneity of the foaming process.

The control of the processing parameters was achieved by means of a PID controller (model X1, Ascon-New England Temperature Solutions, Attleboro, MA, USA) and a syringe pump 500D (Teledyne Isco, Lincoln, NE, USA). A pressure transducer (model P943, Schaevitz-Measurements Specialties, Hampton, VA, USA) was used to measure pressure, and the pressure history

was registered by using a data acquisition system (DAQ PCI6036E, National Instruments, Austin, TX, USA). The pressure release system consists of a discharge valve (model 10-80 NFH, High Pressure Equipment Company, Erie, PA, USA) and a pneumatic electro-valve. The pressure discharge system was designed to allow many different PDRs, from the same P_{sat} , by using different ball valves actuating pressure and/or different downstream piping. There is an on-going debate in the literature on the proper way to describe the shape of the pressure versus time curve.^{4,8} In order to compare the results achieved with different pressure histories and with different apparatuses, to our point of view, the most suitable description and PDR, associated to the different pressure versus time curves, is the maximum value of the curve derivative. A moving average (rolling average or running average) was used over a period of 0.010 s for the depressurization curves obtained with a data acquisition frequency of 1000 Hz. Then, the characteristic PDRs were calculated as the maximum values of the derivative of moving averages.

The experiment procedure is the following: two polymer cylinders, with characteristic size of 1.5 ± 0.1 mm (one of neat *PS* and one of *PS* filled with 1% wt talc), were placed in the minibatch, the vessel was heated to the saturation temperature (T_{sat}) and the pressure was increased up to the saturation pressure (P_{sat}) of 10 MPa. After the solubilization time of 4 h,¹³ during which the P_{sat} and T_{sat} were maintained constant, pressure was quenched to ambient pressure. It is worth noting that in the different tests T_{sat} was always equal to T_{foam} .

The foams were characterized to determine their densities (ρ) and N . ρ was measured according to ASTM D792, using an analytical balance (Mettler Toledo, Columbus, OH, USA). The cellular structure of the foams was investigated by using a scanning electron microscope (SEM-QUANTA 200 3D). The samples were first sectioned with a razor blade in liquid nitrogen and then coated with gold using a sputter coater. N was calculated as $N = \left(\frac{n}{A}\right)^{\frac{3}{2}} \times \left(\frac{\rho_p}{\rho}\right)$, where n is the number of the cells in the area A of the SEM micrograph, and ρ_p is the density of the solid sample.

Results

The bubble nucleation was studied in neat *PS* and talc-filled *PS*. Samples were foamed at three different foaming temperature T_{foam} (i.e. 90°C, 100°C and 110°C), with PDRs ranging from 50 MPa/s to 500 MPa/s. The results were compared in terms of N (calculated as explained in the Materials and methods section) as function of PDR.

The results of N as function of PDR at T_{foam} 90°C are shown in Figure 1(a), comparing the talc-filled *PS* (black-filled rhombs)/neat *PS* (empty rhombs). N increases linearly in a bi-logarithmic scale as a function of PDR. In particular, for neat *PS* foams N increases from $1.4 \cdot 10^7$ cells/cm³ to $6.6 \cdot 10^7$ cells/cm³, and for talc-filled *PS* from $2.5 \cdot 10^9$ cells/cm³ to $8.5 \cdot 10^9$ cells/cm³. The nucleating effect of

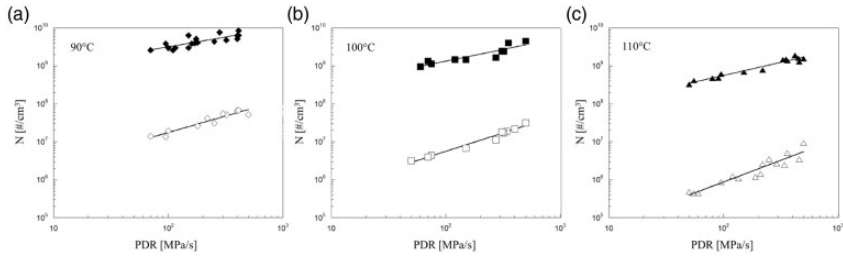


Figure 1. (a) N of neat PS foams (\diamond) and of talc-filled PS foams (\blacklozenge) as function of PDR at 90°C, (b) N of neat PS foams (\square) and of talc-filled PS foams (\blacksquare) as function of PDR at 100°C, (c) N of neat PS foams (\triangle) and of talc-filled PS foams (\blacktriangle) as function of PDR at 110°C. The solid lines are obtained by interpolation with $N = a * PDR^b$ (see text for details).

talc is confirmed by the increase of two order of magnitude on N , through all PDR range.^{14,15} The data are well fitted by using the equation $N = a * PDR^b$ (solid line in Figure 1) The slope b , in a logarithmic scale, is smaller for the talc-filled PS samples.¹⁶ The value of b is a good indication of the activation energy for the bubble nucleation.^{17–19} In the Figure 1(b) and (c) the results of N as function of PDR for T_{foams} equal to 100°C and 110°C are shown for both talc-filled and neat PS samples. At all the temperatures under investigation, N increases linearly as a function of PDR in a bi-logarithmic scale. In particular, for neat PS, it increases from $3.1 * 10^6$ cells/cm³ to $3.2 * 10^7$ cells/cm³ at 100°C and from $4.2 * 10^5$ cells/cm³ to $9.3 * 10^6$ cells/cm³ at 110°C, on the other hand, for talc-filled PS, N increases from $9.5 * 10^8$ cells/cm³ to $4.5 * 10^9$ cells/cm³ at 100°C and from $3.2 * 10^8$ cells/cm³ to $1.5 * 10^9$ cells/cm³ at 110°C. It is evident that, the gap between the N for neat PS samples and the talc-filled samples becomes larger as the temperature increases.^{20,21} We can speculated that at higher temperature the energy available for the bubble nucleation is smaller (i.e. for the lower gas concentration), as confirmed by N results, and as a consequence the decrease of the nucleation energy barrier, due to the talc, has a bigger impact at higher temperatures.

However, increasing PDR, the talc effect is reduced as the distance between the curves decreases. This phenomenon becomes more pronounced increasing the foaming temperature.

It is worth noting that the solubilized gas from 90°C to 110°C decreases by 10% (data reported in the supplementary information) and this, of course, affects both the nucleation and the growth. In the underlying literature, the effect of T_{foam} on N has been extensively studied,^{9,10,15,19} and all concurrent effects of temperature on the properties of the specific polymer/blowing agent system of interest in foaming (e.g. polymer viscosity, mutual diffusivity, interfacial tension, specific volume) have been discussed.^{13,22,23} Arora et al.²⁴ reported experimental data on PS foams at different foaming temperatures (equal to the saturation temperatures), keeping the saturation pressure constant. They observed that the cell size increases roughly

exponentially with temperature, while the density decreases linearly. In particular, from a temperature of 90°C to 110°C, the average diameter of the cells increases from 3 to 15 microns. The cell density is proportional to the inverse of the cubic diameter of a bubble. At least for low PDR, the estimation of N as a function of the temperature from Arora's data seems to be in perfect accordance with the data presented in the current work.

In our case, we addressed this one order of magnitude increase of N , as the temperature decreases from 110°C to 90°C, to the increases of the solubilized CO_2 . Concerning the PDR limit above which N reaches a threshold, from the results show in Figure 1 it is evident that the N continues to increase linearly in the entire PDR range analysed. However, the fact that at lower temperature the curve slopes decreases can be the evidence of a plateau at higher PDR as shown by Muratani et al.²⁵

The linear behavior of N as function of PDR on a log-log scale was observed, for the first time, by Taki,⁶ but at lower PDR range (i.e. from 1 to 10 MPa/s). Herein, we extended the PDR range observing the same phenomenon for a PS/ CO_2 solution foamed at different T_{foam} . Furthermore, a theoretical explanation is still under debate and further studies are required to have a complete model to predict this phenomenon.

Figure 2(a) shows the effect of PDR on ρ of neat PS foams and talc-filled PS at 90°C, in the PDR interval ranging from 50 MPa/s up to 500 MPa/s. It is evident that ρ first decreases with the PDR, and then it reaches a plateau value. The same behaviour is observed in Figure 2(b) and (c) for T_{foam} equal to 100°C and 110°C, respectively.

In Figure 2, the density first decreases with PDR, and then it reaches a plateau value for PDR higher than 400 MPa/s ca. It is worth noting that all samples foamed at the same temperature were subjected to all identical saturation process (T_{sat} and P_{sat} are the same for all the samples, see Materials and methods section), which corresponds to an identical initial concentration of the blowing agent. In order to explain the observed different densities at different PDRs, we may observe

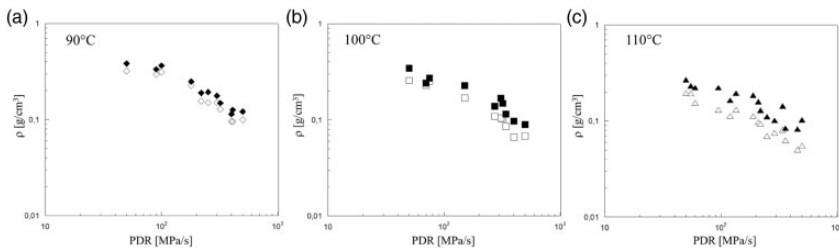


Figure 2. (a) ρ of neat PS foams (\diamond) and of talc-filled PS foams (\blacklozenge) as function of PDR at 90°C, (b) ρ of neat PS foams (\square) and of talc-filled PS foams (\blacksquare) as function of PDR at 100°C, (c) ρ of neat PS foams (\triangle) and of talc-filled PS foams (\blacktriangle) as function of PDR at 110°C.

that, in general, some gas may escape from the polymer/gas solution through the free surface of the sample during the bubble nucleation and growth. Such gas is lost in the surrounding, with a resulting density increase. To assess the effect of PDR on foam density, the following hold true: (i) nucleation is faster, with the increase of the PDR (the thermodynamic instability responsible for the bubble formation is reached earlier); (ii) growth is faster, with the increase of nucleation, since the diffusive path to reach a bubble is shorter and (iii) the effect of gas concentration on diffusion is minor. Hence, the higher the PDR lesser gas may be lost in the surrounding from the free surface.

In Figure 3, characteristic SEM images of samples at different T_{foam} and PDR for neat and talc-filled PS foams are reported. The SEM morphology is in good correlation with what has been shown in Figure 1.

The temperature non-uniformity is very important in polymer foaming processes, strongly affecting the final foam morphologies. The importance of the

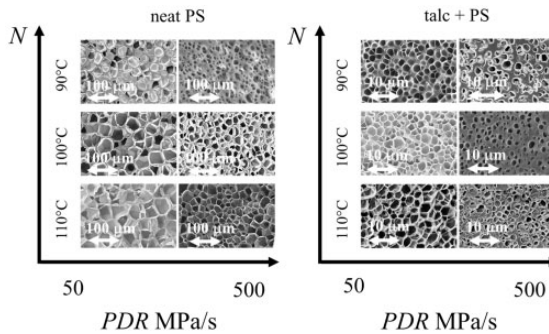


Figure 3. SEM images, showing neat (on the left) and talc-filled (on the right) PS foams morphologies at different PDRs and T_{foam} . Please note the need for using a larger magnification for the cases of talc-filled samples to properly show the foam morphology.

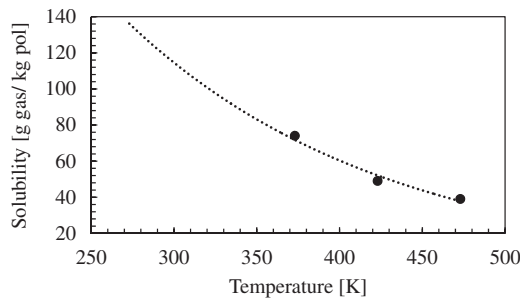


Figure 4. Solubility of CO_2 in PS. The black dots are data from Sato et al.¹³ and the dashed line is an exponential fitting.

non-uniformity in bubble nucleation was studied by SEM observations of foams sections at different PDRs. As it may be observed no bubble size gradient in the foam at different PDRs was detected. We may speculate that, in the minibatch, the dimensions of the samples and of the vessel are small enough to not induce any temperature and PDR local gradients.

Conclusions

In this paper, some insight on bubble nucleation at high PDR and at different foaming temperature (T_{foam}) were discussed. In particular, the increase of PDR and the decrease of T_{foam} improve the bubble nucleation obtaining a finer foam morphology. N increases linearly as a function of PDR in a log-log scale at all T_{foam} investigated (i.e. 90°C, 100°C and 110°C) even at very high PDRs (i.e. up to 500 MPa/s). The effect of talc as nucleating agent does not qualitatively change the effect PDR on N , but decreases the activation energy for the bubble nucleation process.

Declaration of conflicting interests

The author(s) declared no potential conflicts of interest with respect to the research, authorship, and/or publication of this article.

Funding

The author(s) received no financial support for the research, authorship, and/or publication of this article.

Supplementary information

The solubility of CO₂ in PS increases almost linearly with pressure¹³ and in the meantime, it decreases exponentially with the increasing temperature. In the Figure 4, the black dots are the solubility of CO₂ in PS at 10 MPa and at three different temperatures (data obtained from Sato et al.¹³).

The black dashed line is an exponential fitting of the data obtained with the following equation:

$$\text{Solubility} = 782.488 * \exp(-0.006405 * \text{Temperature})$$

The equation was used to estimate the solubility of the gas in the polymer in the current work at different foaming temperatures.

References

1. Colton JS and Suh NP. The nucleation of microcellular thermoplastic foam: Process model and experimental results. *Mater Manuf Process* 1986; 48: 563.

2. Colton JS and Suh NP. The nucleation of microcellular thermoplastic foam with additives: Part I: theoretical considerations. *Polym Eng Sci* 1987; 27: 245.
3. Park CB, Behravesch AH and Venter RD. Low density microcellular foam processing in extrusion using CO₂. *Polym Eng Sci* 1998; 38: 1812.
4. Guo Q, Wang J, Park CB, et al. A microcellular foaming simulation system with a high pressure drop rate. *Ind Eng Chem Res* 2006; 45: 6153.
5. Taki K. Experimental and numerical studies on the effects of pressure release rate on number density of bubbles and bubble growth in a polymeric foaming process. *Chem Eng Sci* 2008; 63: 3643.
6. Park CB, Baldwin DF and Suh NP. Effect of the pressure drop rate on cell nucleation in continuous processing of microcellular polymers. *Polym Eng Sci* 2004; 35: 432.
7. Zel'dovich IAB. Theory of formation of a new phase cavitation. *J Exp Theor Phys* 1942; 12: 525.
8. Khan I, Costeux S, Adrian D, et al. Numerical studies of nucleation and bubble growth in thermoplastic foams at high nucleation rates, 2013, Seattle, WA, SPE FOAMS, Conference proceedings.
9. Khan I, Adrian D and Costeux S. A model to predict the cell density and cell size distribution in nano-cellular foams. *Chem Eng Sci* 2015; 138: 634.
10. Costeux S, Khan I, Bunker SP, et al. Experimental study and modeling of nanofoams formation from single phase acrylic copolymers. *J Cell Plast* 2015; 51: 197.
11. Tammaro D, Contaldi V, Pastore Carbone MG, et al. A novel lab scale batch foaming equipment the mini-batch. *J Cell Plast* 2015; 52: 533–543.
12. Muratani K, Shimbo M and Miyano Y. Correlation of decompression time and foaming temperature on the cell density of foamed polystyrene. *Cell Polym* 2005; 24: 198.
13. Sato Y, Takikawa T, Takishima S, et al. Solubilities and diffusion coefficients of carbon dioxide in poly(vinyl acetate) and polystyrene. *J Supercrit Fluid* 2001; 19: 187.
14. Wang C, Leung SN, Bussmann M, et al. Numerical investigation of nucleating-agent-enhanced heterogeneous nucleation. *Ind Eng Chem Res* 2010; 49: 12783.
15. Wong A and Park CB. The effects of extensional stresses on the foamability of polystyrene–talc composites blown with carbon dioxide. *Chem Eng Sci* 2012; 75: 49.
16. Nelder JA. The fitting of a generalization of the logistic curve. *Biometrics* 1961; 17: 89.
17. Chen L, Sheth H and Wang X. Effects of shear stress and pressure drop rate on microcellular foaming process. *J Cell Plast* 2001; 37: 353.
18. Alvarez-Idaboy JR, Mora-Diez N and Vivier-Bunge A. A quantum chemical and classical transition state theory explanation of negative activation energies in OH addition to substituted ethenes. *J Am Chem Soc* 2000; 122: 3715.
19. Leung SN, Wong A, Park CB, et al. Strategies to estimate the pressure drop threshold of nucleation for polystyrene foam with carbon dioxide. *Ind Eng Chem Res* 2009; 48: 1921.
20. Lee PC, Li G, Lee JWS, et al. Improvement of cell opening by maintaining a high temperature difference in the surface and core of a foam extrudate. *J Cell Plast* 2007; 43: 431.
21. Marrazzo C, Di Maio E and Iannace S. Conventional and nanometric nucleating agents in poly (ϵ -caprolactone) foaming: crystals vs bubbles nucleation. *Polym Eng Sci* 2008; 56: 216.

22. Lee M, Park CB and Tzoganakis C. Measurements and modeling of PS/supercritical CO₂ solution viscosities. *Polym Eng Sci* 1999; 39: 99.
23. Pastore Carbone MG, Di Maio E, Scherillo G, et al. Solubility, mutual diffusivity, specific volume and interfacial tension of molten PCL/CO₂ solutions by a fully experimental procedure: effect of pressure and temperature. *J Supercrit Fluid* 2012; 67: 131.
24. Arora KA, Lesser AJ and Mccarthy TJ. Preparation and characterization of microcellular polystyrene foams processed in supercritical carbon dioxide. *Macromolecules* 1998; 297: 4620.
25. Muratani K, Shimbo M and Miyano Y. Effect of decompression rate and foaming temperature on cell density." In: *conference proceedings, Society of Plastics Engineers, ANTEC, Chicago 2004*, vol. 2, pp. 2674–2678.